 Related Commentary, page 1458

# Vascular endothelium is critically involved in the hypotensive and hypovolemic actions of atrial natriuretic peptide

Karim Sabrane,[1,2] Markus N. Kruse,[1] Larissa Fabritz,[3] Bernd Zetsche,[1] Danuta Mitko,[1] Boris V. Skryabin,[4] Melanie Zwiener,[3] Hideo A. Baba,[5] Masashi Yanagisawa,[6] and Michaela Kuhn[1,2]

[1]Institute of Pharmacology and Toxicology, University of Münster, Münster, Germany. [2]Institute of Physiology, University of Würzburg, Würzburg, Germany. [3]Department of Cardiology and Angiology and [4]Institute of Experimental Pathology, University of Münster, Münster, Germany. [5]Institute of Pathology, University of Duisburg-Essen, Essen, Germany. [6]Department of Molecular Genetics and Howard Hughes Medical Institute, Southwestern Medical Center, Dallas, Texas, USA.

**Atrial natriuretic peptide (ANP), via its vasodilating and diuretic effects, has an important physiological role in the maintenance of arterial blood pressure and volume. Its guanylyl cyclase-A (GC-A) receptor is highly expressed in vascular endothelium, but the functional relevance of this is controversial. To dissect the endothelium-mediated actions of ANP in vivo, we inactivated the *GC-A* gene selectively in endothelial cells by homologous *lox*P/*Tie2*-Cre–mediated recombination. Notably, despite full preservation of the direct vasodilating effects of ANP, mice with endothelium-restricted deletion of the *GC-A* gene (EC *GC-A* KO) exhibited significant arterial hypertension and cardiac hypertrophy. Echocardiographic and Doppler flow evaluations together with the Evan's blue dilution technique showed that the total plasma volume of EC *GC-A* KO mice was increased by 11–13%, even under conditions of normal dietary salt intake. Infusion of ANP caused immediate increases in hematocrit in control but not in EC *GC-A* KO mice, which indicated that ablation of endothelial GC-A completely prevented the acute contraction of intravascular volume produced by ANP. Furthermore, intravenous ANP acutely enhanced the rate of clearance of radio-iodinated albumin from the circulatory system in control but not in EC *GC-A* KO mice. We conclude that GC-A–mediated increases in endothelial permeability are critically involved in the hypovolemic, hypotensive actions of ANP.**

## Introduction

The heart is involved in the regulation of arterial blood pressure (ABP) and blood volume by the secretion of 2 natriuretic peptides (NPs): atrial NP (ANP) and B-type NP (BNP) (1, 2). These NPs activate a common guanylyl cyclase-A (GC-A) receptor expressed in a wide variety of tissues, thereby increasing intracellular cGMP concentrations (3). NPs are secreted from atrial granules into the circulation in response to acute or chronic atrial stretch to act as antihypertensive and antihypervolemic factors via GC-A in distant organs (2, 4). In chronic hemodynamic overload, there is a significant increase in ANP and BNP expression in the cardiac ventricles (1), and in this situation NPs may exert not only endocrine but also local antihypertrophic (ANP) and antifibrotic (BNP) actions (5, 6). The important physiological endocrine role of the ANP/GC-A system in ABP and blood volume homeostasis has been demonstrated in various genetic mouse models. Targeted deletion of the peptide (*ANP*$^{-/-}$) or its receptor (*GC-A*$^{-/-}$), leads to severe, chronic arterial hypertension (7–9) and hypervolemia (10). Remarkably, hypervolemia in *GC-A*$^{-/-}$ mice is apparent even under conditions of normal dietary salt intake (10), which emphasizes the important role of the ANP/GC-A system in not only acute but also chronic regulation of intravascular volume and overall in electrolyte and volume homeostasis. The main known GC-A–mediated hypovolemic actions of ANP include the following: stimulation of renal function, leading to increased natriuresis and diuresis; modulation of transvascular fluid balance by stimulation of microvascular permeability; increased fluid efflux from the intravascular to the lymphatic system within the spleen; inhibition of the renin-angiotensin-aldosterone (RAA) system by direct actions on juxtaglomerular cells and the adrenal glomerulosa; and central nervous system effects that decrease salt appetite and water drinking (reviewed in refs. 2, 4).

The contribution of these different GC-A–mediated actions of ANP to electrolyte and volume homeostasis in vivo is controversial. For instance, although ANP clearly counteracts the RAA system at the level of its expression and function (11), renin and aldosterone levels are not increased in adult *GC-A*$^{-/-}$ mice (12, 13) and despite this, these animals are clearly hypertensive. Thus, the chronic reduction in blood pressure/volume by ANP might be mediated mainly by other actions of the hormone, such as the stimulation of salt and water excretion by the kidneys. However, even very early investigations of human volunteers and intact animals noted that the administration of synthetic ANP in very low doses causes an acute, immediate contraction of intravascular volume that appears to occur well before the ANP-induced urinary losses of fluid and electrolytes (14–18). Even more, this effect is fully preserved in rats with both kidneys and spleen removed and is accompanied by capillary escape

**Nonstandard abbreviations used:** ABP, arterial blood pressure; ACh, acetylcholine; ANP, atrial NP; BNP, B-type NP; BW, body weight; EC *GC-A* KO, endothelium-restricted deletion of the *GC-A* gene; GC-A, guanylyl cyclase-A; HW, heart weight; LVW, left ventricular weight; NP, natriuretic peptide; PE, phenylephrine; RAA, renin-angiotensin-aldosterone; RVW, right ventricular weight; *Tie2-Cre*$^{ki}$ mice, transgenic mice expressing Cre recombinase under the control of the *Tie2* promoter/enhancer.

**Conflict of interest:** The authors have declared that no conflict of interest exists.

**Citation for this article:** *J. Clin. Invest.* **115**:1666–1674 (2005). doi:10.1172/JCI23360.

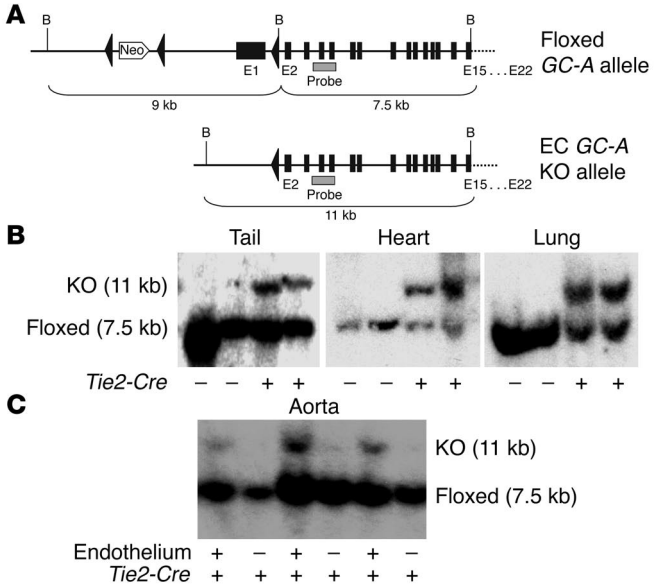


**Figure 1**
Generation and Southern blot characterization of floxed *GC-A* and EC *GC-A* KO mice (**A**) Restriction map of the floxed *GC-A* targeting construct and the *Tie2*-Cre–generated deletion allele. B, *Bam*HI site; Neo, neomycin-resistance cassette; E1–E22, exons 1–22. (**B**) Southern blot analyses of genomic DNA obtained from tails, hearts, lungs, and aortas of floxed *GC-A* and EC *GC-A* KO mice, demonstrating the deletion event that occurs in all tissues from mice harboring the *Tie2-Cre* transgene. The Cre-mediated deletion event abolishes the additional *Bam*HI site inserted in intron 1 by the recombination event. *Bam*HI-digested DNA was hybridized with a specific cDNA probe spanning E2–E6; 11-kb and 7.5-kb bands represent the deletion allele (KO) and targeted allele (Floxed), respectively. (**C**) Southern blot analyses of genomic DNA obtained from isolated aortas of EC *GC-A* KO mice, with (+) and without (–) endothelium; endothelial cells were removed by scraping.

of plasma protein, suggesting that ANP regulates transvascular fluid balance via changes in endothelial permeability (refs. 16–18; comprehensively reviewed in ref. 19).

GC-A is highly expressed on vascular endothelia and ANP binding increases endothelial cGMP levels (20). In the majority of in vitro studies using cultured endothelial cells from large vessels, elevations in cGMP by ANP, NO donors, or cGMP analogs decrease agonist-induced increases in endothelial permeability (21–23). In contrast, in vivo studies using intact rat or frog mesenteric venular microvessels demonstrated that elevations in vascular cyclic GMP content in response to ANP or NO increased microvessel permeability (24). To address this issue in vivo and especially to elucidate to what extent the effect of ANP on endothelial cells plays a role in systemic blood pressure and volume homeostasis, we generated mice with endothelium-restricted deletion of the *GC-A* gene (EC *GC-A* KO). Based on studies in these mice, we conclude that vascular endothelium is critically involved in the acute and chronic moderation of ABP and arterial blood volume by ANP.

## Results

*Generation of EC GC-A KO mice*. Endothelium-specific deletion of *GC-A* was achieved by crossing of mice with floxed *GC-A* (5, 25) with transgenic mice expressing Cre recombinase under the control of the *Tie2* promoter/enhancer (*Tie2-Cre*$^{tg}$ mice) (26). Many recent studies have shown the usefulness of the *Tie2-Cre* transgene in mediating selective and efficient deletion of floxed genes in the endothelial cell lineage; i.e., in macro- and microvascular endothelia (26–28). Accordingly, in mice homozygous for floxed *GC-A*, the *Tie2-Cre* transgene will lead to specific inactivation of *GC-A* in endothelial cells. Indeed, Southern blot analyses of various tissues and isolated aortas from "floxed *GC-A; Tie2-Cre*$^{tg}$" (EC *GC-A* KO) mice showed the deletion event (Figure 1, B and C). After removal of the aortic endothelium, no deletion band could be detected in DNA samples of aortas from EC *GC-A* KO mice, demonstrating endothelial specificity (Figure 1C). Quantitative RT-PCR analysis showed that the expression of *GC-A* mRNA in various tissues from EC *GC-A* KO mice was reduced by 50–70% (Figure 2). Of course, all tissues examined contain many other cell types besides endothelial cells, such as epithelia, myocytes, and interstitial fibroblasts. All these cell types express *GC-A* (2, 4) but only the *GC-A* gene expressed in endothelial cells undergoes *Tie2*-Cre–mediated recombination.

*Vasorelaxing responses to ANP are preserved in isolated arteries from EC GC-A KO mice*. The direct vasorelaxing effects of ANP were evaluated in isolated arterial rings obtained from the thoracic aorta, carotic artery, and pulmonary artery of floxed *GC-A* and EC *GC-A* KO mice. $\alpha_1$-adrenergic contractions elicited by phenylephrine (PE; 10 μM) were stable in all 3 types of arteries and did not differ among genotypes. As shown in Figure 3, in preconstricted arteries from both EC *GC-A* KO mice and control mice with floxed *GC-A*, ANP induced similar rapid and concentration-dependent relaxation. After repeated washout with Krebs buffer, a second PE contraction was obtained in all vessels and the relaxing response to acetylcholine (ACh; 0.1–100 μM) was tested. The endothelium-dependent vasodilator induced concentration-dependent relaxation of all 3 types of arteries tested, up to a 70–80% inhibition of the PE-induced contraction in isolated vessels from floxed *GC-A* and EC *GC-A* KO mice, demonstrating the presence of intact, functional endothelium in these isolated vascular preparations (data not shown). The vasorelaxing effects of ACh also did not differ among genotypes.

*EC GC-A KO mice exhibit salt-resistant hypertension and cardiac hypertrophy*. To ascertain whether deletion of endothelial *GC-A* affects chronic ABP, we subjected conscious mice homozygous for floxed *GC-A* and EC *GC-A* KO mice to ABP measurements using tail cuff

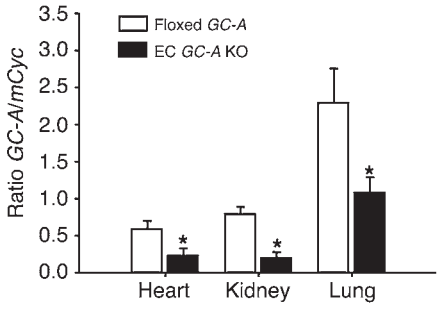


**Figure 2**
Quantitative RT-PCR analyses of *GC-A* mRNA in hearts, kidneys, and lungs from mice with floxed *GC-A* and EC *GC-A* KO mice. Signal intensities were normalized to mouse cyclophilin (*mCyc*). Expression is significantly decreased in EC *GC-A* KO compared with mice with floxed *GC-A* ($n$ = 6 of each tissue and genotype; *$P$ < 0.05 compared with floxed *GC-A*).

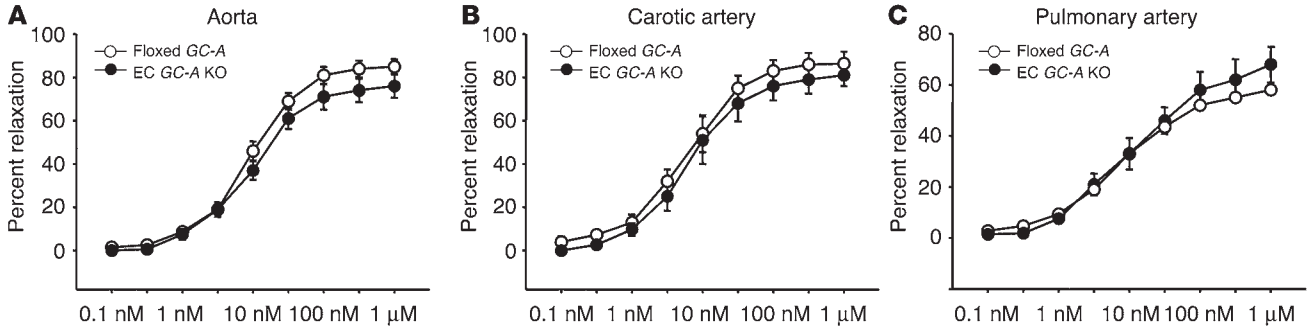


**Figure 3**
Effect of ANP on preconstricted arteries from mice with floxed *GC-A* and EC *GC-A* KO mice. Concentration-response curves. The vasorelaxing effects of ANP are presented as a percentage of the contraction induced by PE (10 μM). $n$ = 8 determinations, corresponding to 8 mice.

plethysmography ($n$ = 60 per genotype). These experiments were carried out on 2- to 6-month-old male and female mice that were fed standard rodent chow (0.6% NaCl). Remarkably, EC *GC-A* KO mice of both sexes displayed significantly increased systolic blood pressure values (by approximately 12–15 mmHg) and diastolic blood pressure values (by approximately 5–10 mmHg) compared with those of their littermates with floxed *GC-A* at all ages studied. Heart rates did not differ significantly between the 2 groups (mice with floxed *GC-A*, 565 ± 12 bpm; EC *GC-A* KO mice, 555 ± 17 bpm). As shown in Figure 4A, in both floxed *GC-A* and EC *GC-A* KO mice, blood pressure and heart rates were not significantly different before and after being fed a low-salt diet for at least 14 days. Thus, dietary salt restriction had no effect on the hypertensive phenotype of EC *GC-A* KO mice. This slight hypertension was associated with significant cardiac enlargement, as indicated by increased ratios of heart weight ([HW], in mg), right ventricular weight ([RVW], in mg) and left ventricular weight ([LVW], in mg) to body weight ([BW], in g) of EC *GC-A* KO mice compared with those of littermates with floxed *GC-A* (all by about 20%; $P < 0.05$; Figure 4B). The cardiac enlargement in EC *GC-A* KO mice fed a normal-salt diet was similar to that of age-matched mice fed a low-salt diet for 2 weeks (Figure 4B). Importantly, ABP levels and HWs of *Tie2-Cre* transgenic mice (control mice not harboring the floxed *GC-A* allele) were not different from those of their wild-type littermates, indicating that endothelial expression of Cre-recombinase per se was not causing the observed cardiovascular changes.

To confirm the cardiac changes at the cellular level, we subjected the dissected ventricles to histological analyses. Morphometrical analyses of PAS-stained sections demonstrated that cell diameters of LV and RV cardiomyocytes from EC *GC-A* KO mice were significantly enlarged compared with those of their littermates with floxed *GC-A* (LV, 15.9 ± 0.8 μm versus 12.6 ± 0.4 μm; RV, 14.7 ± 0.5 μm versus 11.4 ± 0.6 μm, respectively; $P < 0.05$) (Figure 5).

*Chronic hypervolemia in EC GC-A KO mice subjected to normal- or low-salt diet.* To further characterize the cardiac and hemodynamic alterations in EC *GC-A* KO mice, we subjected mice of both genotypes to serial Doppler echocardiographic analyses before (under normal dietary salt conditions) and after 2 weeks of low-salt diet. Corroborating the necropsy data, these analyses showed that EC *GC-A* KO mice had modestly increased LVW/BW ratios, although the difference from mice with floxed *GC-A* by this technique did not reach statistical significance (normal-salt diet, $P = 0.056$; low-salt diet, $P = 0.086$; Figure 6, A and B). LV contractile function was preserved, as indicated by the fractional shortening of the

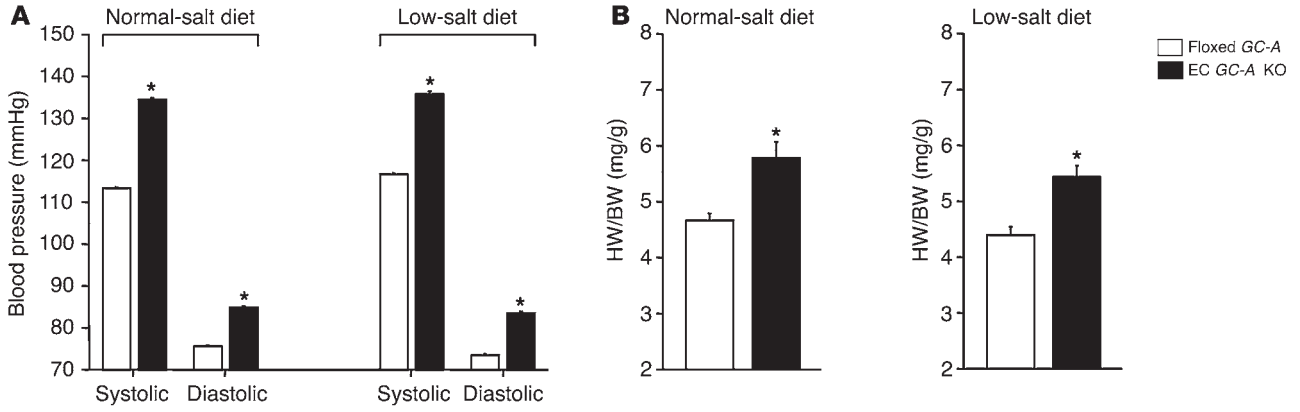


**Figure 4**
Effect of endothelium-restricted disruption of the *GC-A* gene on ABP and cardiac weights. (**A**) Serial systolic and diastolic blood pressure measurements with a tail cuff before (Normal-salt diet) and after 2 weeks of dietary salt restriction (Low-salt diet; $n$ = 16 per genotype). (**B**) HW/BW ratios of age- and sex-matched floxed *GC-A* and EC *GC-A* KO mice under normal-salt and low-salt conditions ($n$ = 20 and 16 per genotype, respectively). *$P < 0.05$ compared with floxed *GC-A*.

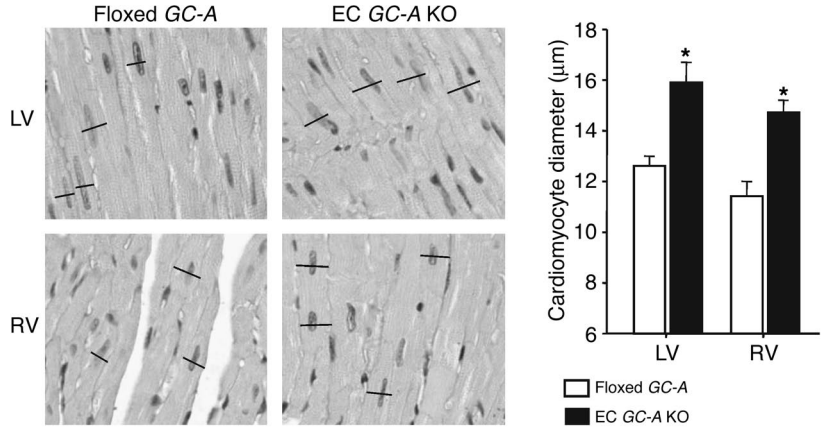


**Figure 5**
Cardiomyocyte diameters in LV and RV ($n = 8$ per genotype; normal-salt conditions; $^*P < 0.05$ compared with floxed *GC-A*). Original magnification, ×200.

LV wall and ejection fraction, which did not differ between genotypes and salt conditions (Figure 6, A and B). Intriguingly, even under normal-salt conditions, cardiac output was increased in EC *GC-A* KO mice by approximately 25% compared with that of control mice with floxed *GC-A* (Figure 6A). In addition, the mean pressure gradient and the maximal flow velocity across the aortic valve were both greater in EC *GC-A* KO mice than in littermates with floxed *GC-A* by 43% and 23%, respectively, with a concomitant increase in stroke volume (Figure 6A). Of note, feeding the mice a low-salt diet had no significant effect on these functional parameters and did not affect their genotype-dependent alterations (Figure 6B). Taken together, these data suggested that EC *GC-A* KO hearts are working with chronically enhanced volume load that is not reduced by dietary salt restriction, at least not at the degree of restriction tested here.

Because Doppler echocardiography provides only an indirect estimation of cardiac output based on blood flow velocity determinations, we wanted to confirm the suspected hypervolemia by measuring plasma volume with the dye Evan's blue (10). Even with a normal-salt diet (0.6% NaCl), plasma volume was greater in EC *GC-A* KO mice than in control mice with floxed *GC-A* by approximately 11–13% ($n = 8$ mice per genotype, all approximately 3 months old; Figure 7A). Notably, this plasma volume expansion was not reversed in mice fed a low-salt diet for 2 weeks (Figure 7B) and was not accompanied by changes in the blood plasma concentration of total proteins and $Na^+$, $K^+$, and $Cl^-$ (see Table 1). Plasma electrolyte concentrations of younger mice (1–2 months) or older mice (4–6 months) also did not differ between genotypes (data not shown).

*EC GC-A KO mice exhibit normal daily $Na^+$/water intake and renal output.* To determine whether the absence of endothelial GC-A modified drinking behavior or renal function as parameters modulating plasma volume, we measured food and water intake as well as urine output of mice in metabolic cages. In mice of both genotypes, urine volume and urinary $Na^+$ excretion were substantially less than water and $Na^+$ intake; this is typical of mice (they have high insensible fluid loss) and has also been observed in other studies (29). As depicted in Table 1, there were no significant differences between genotypes with respect to daily food, water and $Na^+$ intake and urine output or urinary $Na^+$ excretion. In addition, plasma urea and urinary creatinine concentrations were also similar in floxed *GC-A* and EC *GC-A* KO mice, suggesting normal renal function in the latter (Table 1). Because plasma [$Na^+$] and BWs of age-matched adult mice from both genotypes were similar and stable, we conclude

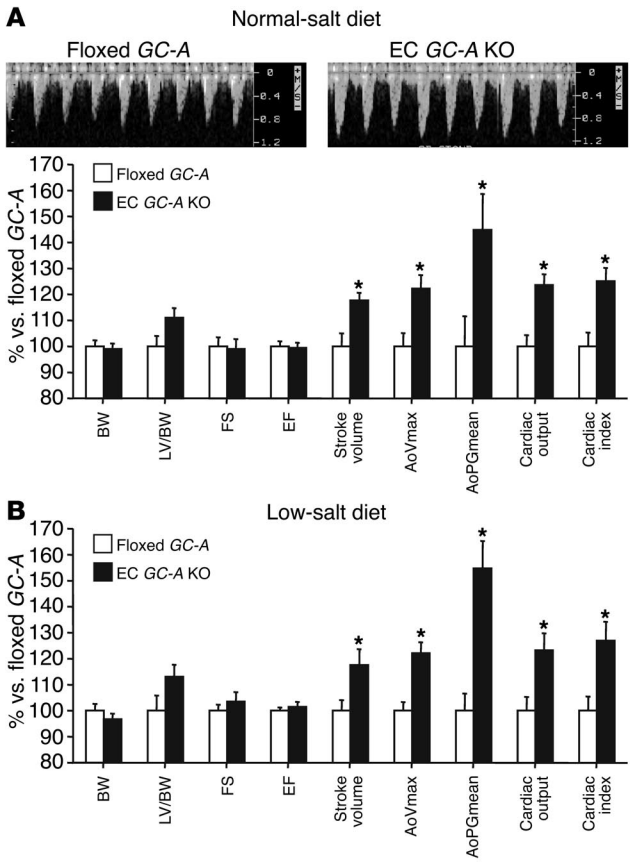


**Figure 6**
Effect of endothelium-restricted disruption of the *GC-A* gene on cardiac function. (**A** and **B**) Serial echocardiographic and Doppler flow parameters of male floxed *GC-A* and EC *GC-A* KO littermates before (Normal-salt diet) (**A**) and after at least 2 weeks of dietary salt restriction (Low-salt diet) (**B**). Mice of both genotypes were assessed at comparable heart rates (402 ± 12 versus 434 ± 11 bpm). (**A**) Top: Representative examples of aortic flow profiles of a mouse with floxed *GC-A* and an EC *GC-A* KO mouse at the same heart rate. Flow undulates slightly with breathing. Abbreviations and calculations are as follows: BW, in g; LV/BW, ratio of LVW (in mg) to BW (in g); LVW, calculated as described in ref. 10; FS, fractional shortening; EF, ejection fraction; AoVmax, in m/s, maximal blood flow velocity across the aortic valve; AoPGmean, in mmHg, mean pressure gradient of blood flow across the aortic valve; stroke volume, in μl; cardiac output, in ml/min, calculated as stroke volume × HR; cardiac index, calculated as cardiac output/BW. Transvalvular and jugular Doppler measurements rendered comparable results. Parameters were calculated as described in ref. 10 ($n = 16$ per genotype; $^*P < 0.05$ compared with floxed *GC-A*).

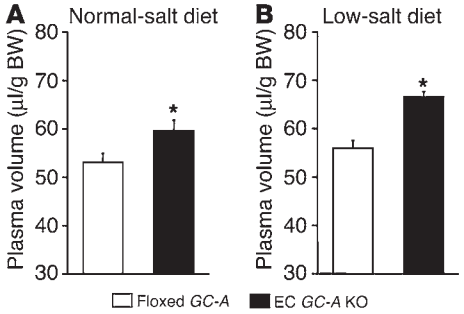


**Figure 7**
Effect of endothelium-restricted disruption of the *GC-A* gene on plasma volume. (**A** and **B**) Plasma volume in male floxed *GC-A* and EC *GC-A* KO littermates fed either a normal-salt diet (**A**) or a low-salt diet (**B**) was determined by the Evan's blue dilution technique ($n$ = 8 mice per genotype and condition; *$P$ < 0.05 compared with floxed *GC-A*).

that EC *GC-A* KO mice were volume-expanded in a steady state with respect to tonicity and volume without apparent changes in renal $Na^+$/water excretion or in oral $Na^+$/water intake.

*Acute effects of exogenous ANP on hematocrit are abolished in EC GC-A KO mice*. To study the contribution of endothelial GC-A to the acute reduction of plasma volume by ANP, we tested the effect of exogenous ANP administration on hematocrit. Baseline hematocrit values did not differ between genotypes (Table 1). Infusion of ANP at a dose of 500 ng/kg BW/min to mice with floxed *GC-A* caused a significant, immediate increase in hematocrit, indicating an acute contraction of plasma volume. Similar effects of ANP have been reported in many other experimental studies (14–17). In contrast, ANP-infusion had no effect at all on the hematocrit of EC *GC-A* KO mice (Figure 8).

*Acute effects of exogenous ANP on microvascular albumin permeability are abolished in EC GC-A KO mice*. To examine the in vivo role of endothelial GC-A in transvascular albumin flux, we gave male age-matched EC *GC-A* KO mice and littermates with floxed *GC-A* tail vein injections of [$^{125}$I]BSA. Blood samples were obtained at various time points and the rate of clearance for radio-iodinated BSA was determined. As shown in Figure 9A, in vehicle-infused mice of both genotypes, only a small fraction (about 10%) of the iodinated BSA was cleared from the circulation within the 15-minute observation period. Infusion of ANP at a dose of 500 ng/kg BW/min to mice with floxed *GC-A* caused a significant increase in the clearance rate of iodinated BSA: the level of iodinated BSA in the circulatory system decreased by approximately 20% at 5 minutes and by approximately 40% at 15 minutes of infusion. In contrast, ANP infusion failed to stimulate BSA clearance in EC *GC-A* KO mice (Figure 9A). As a result, the levels of iodinated BSA in the circulatory system of the EC *GC-A* KO mice at 15 minutes of ANP infusion were significantly greater than the levels seen in littermates with floxed *GC-A*.

At 30 minutes of ANP infusion, the mice were euthanized and various tissues were isolated for determination of the amount of iodinated BSA that accumulated in a given tissue. These results are shown graphically in Figure 9B; the percent differences between the levels of iodinated BSA in the EC *GC-A* KO mice and mice with floxed *GC-A* are compared. Note that all of the tissues examined showed less accumulation of BSA in EC *GC-A* KO mice than their control littermates with floxed GC-A (up to 60% less in jejunum, colon, and skeletal muscle). Of course, measurements of albumin accumulation in tissues represent both extravascular leakage and the albumin that is retained in the microcirculation. However, together with the plasma clearance studies, these results indicate that the increases in vascular permeability in response to ANP occur at the microvascular level and affect the permeability even for macromolecules such as albumin. These responses are apparently abolished in EC *GC-A* KO mice.

## Discussion

The present study has described selective inactivation of the GC-A receptor for ANP in the endothelial cell lineage using the *lox*P/*Tie2*-Cre system. The direct vasorelaxing effects of ANP on isolated arteries of EC *GC-A* KO mice were fully preserved. Despite this, these mice exhibited mild but significant chronic hypertension, hypervolemia, and global cardiac hypertrophy. Remarkably, these phenotypical features were observed even under conditions of normal dietary salt intake and were not affected by dietary salt restriction. Furthermore, the acute increases in microvascular albumin permeability and reductions in plasma volume elicited by exogenous synthetic ANP in control mice were totally prevented in EC *GC-A* KO littermates. We conclude that GC-A/cGMP–dependent modulation of microvessel endothelial permeability is critical to both the acute and chronic hypovolemic actions of ANP.

Within the vascular system, *GC-A* is densely expressed on both smooth muscle cells and endothelia. Remarkably, smooth muscle–restricted deletion of *GC-A* in mice completely abolished the direct vasodilating effects of ANP but did not affect resting ABP (25). In contrast, endothelium-restricted *GC-A* deletion preserved ANP vasodilatation but caused hypertension. Physiological and Doppler echocardiography studies showed that EC *GC-A* KO mice had chronic hypervolemia, with the total plasma volume being expanded by 11–13%. By comparison, in mice of the same genetic background harboring global, systemic *GC-A* deletion, plasma volume is chronically increased by approximately 30% (10). We conclude that vascular endothelium mediates in a significant part the long-term balance of intravascular

**Table 1**
Metabolic balance data and hematocrit

| | Floxed *GC-A* | EC *GC-A* KO |
|---|---|---|
| Body weight (g) | 26.6 ± 1.3 | 26.5 ± 1.2 |
| Plasma [$Na^+$] (mmol/l) | 146.1 ± 2.3 | 147.6 ± 1.8 |
| Plasma [$K^+$] (mmol/l) | 6.7 ± 0.9 | 6.0 ± 0.9 |
| Plasma [$Cl^-$] (mmol/l) | 113.5 ± 2.3 | 113.9 ± 2.1 |
| Plasma [urea] (mg/dl) | 20.5 ± 3.4 | 19.2 ± 2.6 |
| Plasma [protein] (g/dl) | 6.2 ± 0.1 | 6.1 ± 0.1 |
| Hematocrit (%) | 43.3 ± 1.1 | 41.0 ± 1.1 |
| Urine volume (μl/g/day) | 28.0 ± 3.8 | 30.2 ± 4.9 |
| Urine [$Na^+$] (mmol/l) | 142.0 ± 19.5 | 114.0 ± 19.6 |
| Urine [$K^+$] (mmol/l) | 597.0 ± 91.7 | 500.6 ± 62.7 |
| Urine [creatinine] (mg/dl) | 73.3 ± 4.7 | 71.2 ± 5.7 |
| Water intake (μl/g/day) | 124.3 ± 12.9 | 139.9 ± 14.1 |
| Food intake (mg/g/day) | 101.0 ± 10.6 | 92.7 ± 8.6 |
| Daily total $Na^+$ intake (μg/g/day) | 205.1 ± 21.4 | 188.8 ± 17.2 |
| Daily urinary $Na^+$ excretion (μg/g/day) | 91.2 ± 15.4 | 73.1 ± 10.4 |

Data are from approximately 3-month-old floxed *GC-A* and EC *GC-A* KO mice on a normal-salt diet ($n$ = 11 per group).

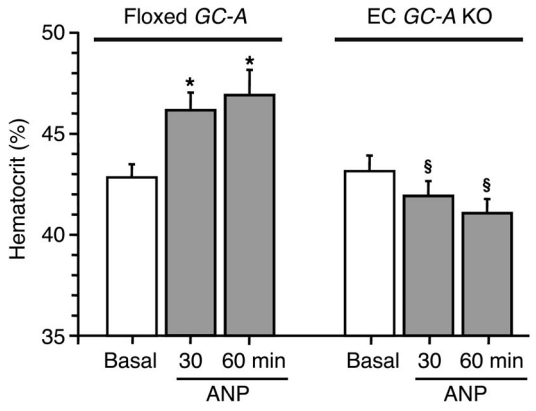


**Figure 8**
Effect of i.v. ANP (500 ng/kg BW/min, as an infusion) on hematocrit values of awake floxed *GC-A* and EC *GC-A* KO mice. Note that at 30 and 60 minutes of ANP infusion, mice with floxed *GC-A* show marked increases in hematocrit. Notably, this effect was completely abolished in EC *GC-A* KO mice ($n = 8$ per genotype; $^*P < 0.05$ compared with basal; $^§P < 0.05$ compared with floxed *GC-A*).

blood volume by ANP. As shown, the blood plasma concentration of total proteins and electrolytes in EC *GC-A* KO mice were not different from control littermates with floxed GC-A. Also, BWs were not different from those of their control littermates, indicating that total body fluid volume was not altered. Taken together, these observations suggest that the chronic increase in plasma volume in EC *GC-A* KO mice was accounted for by a respective decrease in interstitial fluid volume. Based on these observations, we suggest that endothelial GC-A is critically involved in the chronic maintenance of transvascular fluid balance. Abolition of the endothelial ANP effects, probably by a reduction in basal microvascular macromolecule permeability (ref. 19; and see below), shifts the balance of hydrostatic and colloid osmotic forces across capillary walls in favor of moving protein-free fluid from interstitial pools into the plasma and ultimately increases intravascular volume.

The kidneys, spleen, and central nervous system are other important sites mediating the hypovolemic actions of ANP (4). Because EC *GC-A* KO mice have unchanged daily urine/$Na^+$ output and plasma urea concentrations as compared to control littermates with floxed GC-A, altered renal function is unlikely to be the primary cause of their chronic hypervolemia. However, it is indeed intriguing that kidney function was not able to compensate for pressure/volume overload. Our future studies will be directed toward addressing this question and specifically toward elucidating the role of renal endothelial ANP effects. Within the spleen, ANP stimulates fluid extravasation into the lymphatic system by raising intrasplenic microvascular pressure (30). ANP causes vasoconstriction in the splenic vasculature (of veins more than of arteries) by an endothelium-independent mechanism, mediated by GC-A (31). Changes in capillary endothelial permeability seem not to be involved. The splenic capillary beds have a discontinuous endothelium (32) and are freely permeable to plasma proteins (33); i.e., there is no colloid osmotic gradient across the capillary wall to oppose fluid efflux, and modest increases in splenic microvascular hydraulic pressure are able to induce a significant increase in fluid extravasation (30). Thus, although the spleen is an important site of ANP-induced fluid extravasation, this action of ANP is not mediated by the endothelium and therefore is unlikely to be compromised in EC *GC-A* KO mice. Finally, central nervous system effects that decrease salt appetite and water drinking are also involved in the chronic hypovolemic actions of ANP (34). As shown here, spontaneous daily water and $Na^+$ intake apparently was not altered in EC *GC-A* KO mice and therefore cannot account for the observed hypervolemia.

Of note, the blood pressure and plasma volume in EC *GC-A* KO mice remained elevated and unchanged in response to dietary salt restriction, indicating salt-resistant hypertension and hypervolemia. This phenotype, although somehow unexpected, is in fact consistent with the phenotype of mice with global, systemic disruption of the *GC-A* gene (8, 9). In contrast, disruption of the gene encoding ANP leads to a salt-sensitive form of hypertension (7). An explanation for the acquisition of salt sensitivity in *ANP* gene–deficient animals but not in *GC-A* gene–deficient animals remains unresolved (comprehensively discussed in ref. 35).

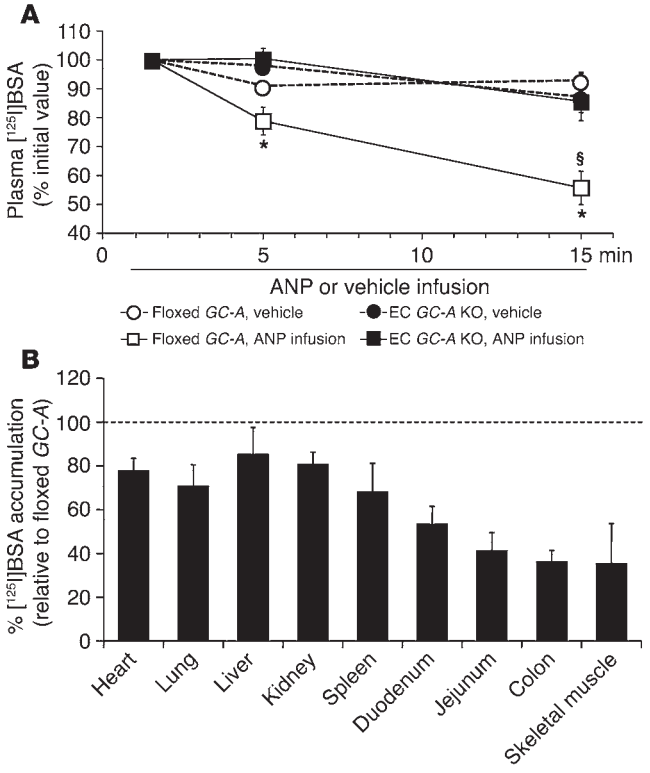


**Figure 9**
Effect of i.v. ANP (500 ng/kg BW/min, as infusion) on the rate of [$^{125}$I]BSA clearance from the circulatory system of awake floxed *GC-A* and EC *GC-A* KO mice. (**A**) Plasma clearance of iodinated BSA. Note that at 5 and 15 minutes of ANP infusion, mice with floxed *GC-A* show approximately 20% and 40% clearance of the iodinated BSA ($n = 8$). In contrast, less than 10% of the iodinated BSA was cleared at these time points in ANP-infused EC *GC-A* KO mice ($n = 8$) or in vehicle-infused mice of either genotype ($n = 2$ per genotype). (**B**) Tissue accumulation of iodinated BSA. Various tissues from EC *GC-A* KO mice, especially intestinal segments and skeletal muscle, show diminished accumulation of [$^{125}$I]BSA after ANP infusion, compared with tissues from mice with floxed *GC-A* (set at 100%). $^*P < 0.05$ compared with vehicle; $^§P < 0.05$ compared with EC *GC-A* KO.

ANP regulates arterial blood volume not only chronically but also in an acute fashion, for instance, in situations of acute volume expansion or sudden increases in blood pressure that cause the release of atrial granules from the heart (1, 4, 36). In fact, increased atrial wall tension produced by volume expansion is the dominant stimulus for ANP release, and the ANP/GC-A signaling pathway has often been thought of as an acute sensor of changes in blood volume (36). To study the role of endothelial GC-A in the acute regulation of intravascular volume, we mimicked the sudden cardiac release of ANP by i.v. application of synthetic peptide. As shown, in awake mice with intact endothelial GC-A, exogenous ANP caused an immediate and marked increase in hematocrit that, according to many previous studies (14–17), results from acute contraction of intravascular plasma volume. Remarkably, this effect was completely abolished in EC *GC-A* KO mice, demonstrating that the presence of endothelial GC-A is an absolute prerequisite for this action of ANP to occur. Together with earlier observations in nephrectomized animals (16, 17), our study provides final proof of the concept that the acute hypovolemic effect of ANP cannot be fully explained by renal losses in fluid and electrolytes. The most likely mechanism is a change in capillary permeability and, thereby, in transcapillary exchange of fluid. To further investigate this issue, we injected radio-iodinated BSA into EC *GC-A* KO mice and compared its rate of clearance from the circulatory system with that of control mice with floxed *GC-A*. In accordance with published studies (18), ANP infusion markedly increased [$^{125}$I]BSA extravasation in control mice. In EC *GC-A* KO mice this effect was totally absent, demonstrating that the ANP-induced acute increases in capillary permeability for macromolecules such as albumin are mediated by endothelial GC-A. Thus, ANP/GC-A–induced plasma protein escape across capillary walls increases interstitial oncotic pressure and ultimately can shift fluid from the intravascular to the interstitial compartment in an acute, immediate fashion.

Which cellular pathways mediate the effects of ANP on endothelial permeability? Microvascular permeability for macromolecules such as albumin is mediated by both caveolar transcytosis across endothelial cells and paracellular movement. It has been shown that endothelial NO, which also signals via cGMP in endothelial cells, increases vascular permeability by regulating the paracellular pathway (37). The exact mechanism of how cGMP regulates vascular permeability is poorly understood, but might involve cAMP levels in endothelial cells. He et al. have shown that increased cGMP stimulates phosphodiesterase 2 and lowers cAMP, resulting in $[Ca^{2+}]_i$-independent increases in permeability in rat and frog mesenteric vessels (24, 38). Another possible action of cGMP is through its ability to stimulate cGMP-dependent protein kinase and thereby the phosphorylation of VASP, a protein associated with focal adhesion sites and adherens junctions (39). However, the exact role that VASP plays in regulating vascular permeability and how this and/or cAMP-dependent pathways are affected by ANP/GC-A/cGMP signaling in endothelial cells is not known and will be an issue for our future studies.

In conclusion, the present study has demonstrated that endothelial GC-A is critically involved in both the acute and chronic hypovolemic actions of ANP. It is also the first to our knowledge to describe hypertension and hypervolemia resulting from deficiency of a single receptor in endothelial cells. Modulation of endothelial permeability may in fact represent one of the physiologically most important actions of ANP. Endothelial dysfunction is one of the earliest consequences of chronic arterial hypertension in patients (40). It is not known whether these endothelial changes also affect responsiveness to ANP. Our studies of EC *GC-A* KO mice have indicated that an inhibition of the endothelial ANP effects would accelerate the progression of the disease and support further work to assess the importance of the ANP/GC-A system, particularly its endothelial alterations, in human cardiovascular diseases.

## Methods

*Generation of EC GC-A KO mice*. Endothelium-selective deletion of *GC-A* was achieved by the *lox*P/Cre recombination system. We previously reported the generation and characterization of mice homozygous for floxed *GC-A* (5, 25). A neomycin-resistance cassette flanked by 2 *lox*P sites was placed 2.6 kb from exon 1, upstream from the promoter region of *GC-A*. A third *lox*P sequence was placed in intron 1, introducing a new *Bam*HI site for later genotyping. Thus, the promoter region and exon 1 (encoding the signal peptide) were flanked by *lox*P sites (Figure 1A). As demonstrated previously, expression and function of the floxed *GC-A* gene is not different from that of wild type (5, 25). However, Cre recombinase–mediated deletion of the floxed *GC-A* gene is sufficient to inactivate GC-A function completely (5, 25). For selective deletion of *GC-A* in vascular endothelium, mice with floxed *GC-A* were mated with *Tie2-Cre*$^{tg}$ mice (26). The efficiency and specificity of the *Tie2*-driven, Cre-mediated deletion of floxed genes in macro- and microvascular endothelia has been demonstrated in many previous studies (27, 28). Male and female mice homozygous for floxed *GC-A* and heterozygous for the *Tie2-Cre* transgene (EC *GC-A* KO) aged 3–5 months were used. Their littermates with floxed *GC-A* (with normal *GC-A* expression levels) served as controls. Mice were on a mixed genetic background (129/Sv×C57BL/6) and received standard rodent chow (0.7% NaCl; Altromin). All experiments were approved by the Bezirksregierung in Münster, Germany, and were performed in accordance with NIH guidelines.

*Genotyping by PCR and Southern blot analyses of genomic DNA*. DNA from tail tip biopsies and various tissues was extracted in phenol/chloroform and was ethanol precipitated. For PCR, the *Tie2-Cre* transgene was detected by using primers within the *Tie2* promoter and Cre-coding region (Tie2-YZ 101, 5′-CCCTGTGCTCAGACAGAAATGAGA-3′; Tie2-YZ 98, 5′-CGCATAACCAGTGAAACAGCATTGC-3′) (26). The floxed *GC-A* allele and its Cre-mediated recombination were detected using a combination of 3 oligonucleotide primers as recently described (10). Southern blot analyses were carried out as described previously (5, 25) (see Figure 1 legend).

*Quantification of GC-A mRNA expression by real-time RT-PCR*. Quantitative analysis of *GC-A* mRNA expression in various tissues obtained from floxed *GC-A* and EC *GC-A* KO mice was performed by RT-PCR using the LightCycler Detection System (Roche Diagnostics) as previously described (25). Quantitative PCR analysis was performed using the LightCycler Software (Roche Diagnostics). GC-A transcripts were normalized to mouse cyclophilin.

*In vitro studies of vascular tone*. Ring segments of the descending thoracic aorta (luminal diameter 2,000–2,200 μm), pulmonary artery (luminal diameter 1,000–1,200 μm) and carotic artery (luminal diameter 200–400 μm) were mounted in a myograph (model 410A; J.P. Trading) for recording of isometric wall tension (25). After a 15-minute equilibration in 37°C, oxygenated (95% $O_2$ and 5% $CO_2$) Krebs-Ringer bicarbonate buffer, rings were contracted with PE (10 μM; Sigma-Aldrich), and cumulative concentrations of mouse ANP (Bachem) and ACh (Sigma-Aldrich) were tested.

*Blood pressure measurements*. Systolic and diastolic blood pressure and heart rate were measured in conscious mice ranging from 2 to 6 months of age by a noninvasive tail-cuff method (Softron) between 10:00 and 12:00 as described previously (13, 25). For study of the effects of dietary

salt intake, in a subgroup of approximately 3-month-old male animals, blood pressure and echocardiographic measurements were first obtained in mice fed normal salt chow (0.6% NaCl; final net $Na^+$ concentration, 0.2%). Animals were then fed a low-salt diet (0.13% NaCl; final net $Na^+$ concentration, less than 0.05%) for an additional 2 weeks and parameters were remeasured within the third week ($n$ = 16 per genotype). All food was from Altromin; tap water was provided ad libitum.

*Echocardiography and Doppler flow studies*. Serial LV M-mode and Doppler flow measurements were carried out in diazepame-sedated (17.5 mg/kg BW i.p.) floxed *GC-A* and EC *GC-A* KO littermates before (on a normal-salt diet) and after at least 2 weeks of a low-salt diet ($n$ = 16). Measurements of LV diameters, indices of contractility, and flow were conducted using a digital Doppler echocardiography system (Philips Sonos 5500) equipped with a 15-MHz linear transducer for 2-dimensional and M-mode imaging and a 12-MHz sector scanner for Doppler measurements. Doppler echocardiography was performed both from an apical approach and from the jugulum in order to ensure reproducibility (see Figure 6A legend) (10).

*Plasma volume determinations*. The plasma volumes of age- and sex-matched mice on a normal-salt (0.6% NaCl) versus a low-salt diet (0.13% NaCl for at least 2 weeks) were determined with the Evan's blue dilution method as described previously (10). Evan's blue dye (Sigma-Aldrich; 1 μl/g BW of a solution of 0.5% weight/volume in sterile isotonic saline) was injected via a tail vein. Five minutes later the mice were anesthetized with urethane (2 g/kg BW, i.p.) and additional 5 minutes later they were sacrificed and blood was collected by cardiac puncture for determination of circulating Evan's blue levels (10). The hearts were dissected and analyzed as described below.

*Determination of cardiac weights and cardiomyocyte diameters*. The hearts were weighed and the atria and RV free wall were dissected away from the LV inclusive of the septum. The individual chambers were weighed and fixed in 4% buffered formaldehyde. Ventricles were embedded in paraffin, and 5-μm sections were stained with hematoxylin and eosin or with PAS (to discriminate cardiomyocyte cell borders). Photomicrographs of the sections were evaluated by a computer-assisted image analysis system (Olympus BX41) using analySIS software (SIS) (5, 13) by investigator blinded to the genotypes. The mean cardiomyocyte diameters were calculated by measurement of approximately 100 cells per specimen (8 hearts per genotype) in the region of the cell nucleus (5, 13).

*Metabolic balance studies*. Mice were acclimated to metabolic cages (Techniplast) for 24 hours before data collection. They received a standard rodent chow (0.6% NaCl) and water ad libitum. Urine output and water intake were monitored for additional 24 hours; urine was collected under mineral oil. The mice were then euthanized, blood samples were collected by cardiac puncture in lithium-heparin–coated tubes, and plasma as well as urine was analyzed for total protein, urea, creatinine, $Na^+$, $K^+$, and $Cl^-$ concentrations (System Vitros 250 Chemistry; Johnson & Johnson).

*Acute effects of exogenous ANP on hematocrit*. For prevention of confounding factors associated with anesthesia, this and the following invasive studies were conducted in conscious mice with an indwelling jugular catheter (25). Synthetic mouse ANP was infused with 500 ng/kg BW/min (2.5 μl/kg BW/h) for 60 minutes via a microinfusion pump (Harvard Apparatus). Control mice received vehicle (saline) at the same volume rate. Hematocrit was measured before and at 30 and 60 minutes of infusion by collection of a drop of blood into a hematocrit capillary via a tail vein and by spinning it in a microfuge.

*Acute effects of ANP on in vivo vascular permeability for [$^{125}$I]albumin*. Mice received a jugular vein catheter as described above. Two days later, 15 μCi of [$^{125}$I]BSA (Immundiagnostik) in 15 μl of phosphate-buffered saline was introduced into awake mice via tail vein injection. A first blood sample was then collected from a tail vein at 2 minutes after injection (starting point, see below). Infusion of ANP or vehicle via the jugular cannula was initiated immediately after (dosage and infusion rate as above) and additional venous blood samples were then collected from the tail at 5 and 15 minutes of infusion (7 and 17 minutes after injection of [$^{125}$I]BSA). The amount of radioactivity in 10 μl of plasma was determined using a γ-counter. The clearance rate for each mouse was calculated by using the number of cpm obtained from the 2-minute time point as starting point, i.e., 100% (37), as shown graphically in Figure 9A. At 30 minutes after injection, the mice were euthanized and various organs were isolated. The tissues were washed thoroughly in phosphate-buffered saline to remove as much residual blood as possible. The amount of [$^{125}$I]BSA in each tissue sample was then determined. Each tissue sample was weighed, and the amount of radioactivity in a given tissue sample was expressed as cpm/g (37).

*Data analysis*. Results are shown as the mean ± SEM. Differences between EC *GC-A* KO mice and mice with floxed *GC-A* were evaluated with an unpaired Student's $t$ test. The serial changes in blood pressure and Doppler echocardiographic parameters before/after low-salt diet and of hematocrit and [$^{125}$I]BSA clearance before and during ANP infusion were analyzed by a repeated-measures ANOVA followed by Bonferroni and Student-Newman-Keuls post-hoc test for multiple comparisons. $P$ values of less than 0.05 were considered statistically significant.

## Acknowledgments

This work was supported by the Deutsche Forschungsgemeinschaft (grants KU 1037/3-1 and KU 1037/4-1) and Interdisziplinares Zentrum fur Klinische Forschung. K. Sabrane received a doctoral stipend from the Innovative Medizinische Forschung (IMF; Münster, Germany). M. Kuhn would like to thank Stefan Silbernagl (Institute of Physiology, University of Würzburg) for his continuous support.

Received for publication September 15, 2004, and accepted in revised form March 8, 2005.

Address correspondence to: Michaela Kuhn, Physiologisches Institut der Universität Würzburg, Röntgenring 9, D-97070 Würzburg, Germany. Phone: 49-931-31-2721; Fax: 49-931-31-2741; E-mail: michaela.kuhn@mail.uni-wuerzburg.de.

Karim Sabrane, Markus N. Kruse, and Larissa Fabritz contributed equally to this work.

1. De Bold, A.J., et al. 2001. The physiological and pathophysiological modulation of the endocrine function of the heart. *Can. J. Physiol. Pharmacol.* **79**:705–714.
2. Kuhn, M. 2003. Structure, regulation, and function of mammalian membrane guanylyl cyclase receptors, with a focus on guanylyl cyclase-A. *Circ. Res.* **93**:700–709.
3. Drewett, J.G., and Garbers, D.L. 1994. The family of guanylyl cyclase receptors and their ligands. *Endocr. Rev.* **15**:135–162.
4. Brenner, B.M., Ballermann, B.J., Gunning, M.E., and Zeidel, M.L. 1990. Diverse biological actions of atrial natriuretic peptide. *Physiol. Rev.* **70**:665–699.
5. Holtwick, R., et al. 2003. Pressure-independent cardiac hypertrophy in mice with cardiomyocyte-restricted inactivation of the atrial natriuretic peptide receptor guanylyl cyclase-A. *J. Clin. Invest.* **111**:1399–1407. doi:10.1172/JCI200317061.
6. Tamura, N., et al. 2000. Cardiac fibrosis in mice lacking brain natriuretic peptide. *Proc. Natl. Acad. Sci. U. S. A.* **97**:4239–4244.
7. John, S.W., et al. 1996. Blood pressure and fluid-electrolyte balance in mice with reduced or absent ANP. *Am. J. Physiol.* **271**:R109–R114.
8. Lopez, M.J., et al. 1995. Salt-resistant hypertension in mice lacking the guanylyl cyclase-A receptor for atrial natriuretic peptide. *Nature.* **378**:65–68.
9. Oliver, P.M., et al. 1997. Hypertension, cardiac hypertrophy, and sudden death in mice lacking natriuretic peptide receptor A. *Proc. Natl. Acad. Sci. U. S. A.* **94**:14730–14735.
10. Skryabin, B.V., et al. 2004. Hypervolemic hypertension in mice with systemic inactivation of the (floxed) guanylyl cyclase-A gene by alphaMHC-Cre-mediated recombination. *Genesis.* **39**:288–298.

11. Johnston, C.I., et al. 1989. Interaction between atrial natriuretic peptide and the renin angiotensin aldosterone system. Endogenous antagonists. *Am. J. Med.* **87**:24S–28S.
12. Shi, S.J., Nguyen, H.T., Sharma, G.D., Navar, L.G., and Pandey, K.N. 2001. Genetic disruption of atrial natriuretic peptide receptor-A alters renin and angiotensin II levels. *Am. J. Physiol.* **281**:F665–F673.
13. Holtwick, R., et al. 2002. Left but not right cardiac hypertrophy in atrial natriuretic peptide receptor-deficient mice is prevented by angiotensin type 1 receptor antagonist losartan. *J. Cardiovasc. Pharmacol.* **40**:725–734.
14. Biollaz, J., Nussberger, J., Waeber, B., and Brunner, H.R. 1986. Clinical pharmacology of atrial natriuretic (3-28)eicosahexapeptide. *J. Hypertens.* **4**(Suppl. 2):101–108.
15. Richards, A.M., et al. 1988. Low dose infusions of 26- and 28-amino acid human atrial natriuretic peptides in normal man. *J. Clin. Endocrinol. Metab.* **66**:465–472.
16. Flückiger, J.P., et al. 1986. Effect of atriopeptin III on hematocrit and volemia of nephrectomized rats. *Am. J. Physiol.* **251**:H880–H883.
17. Almeida, F.A., Suzuki, M., and Maack, T. 1986. Atrial natriuretic factor increases hematocrit and decreases plasma volume in nephrectomized rats. *Life Sci.* **39**:1193–1199.
18. Zimmerman, R.S., Trippodo, N.C., MacPhee, A.A., Martinez, A.J., and Barbee, R.W. 1990. High-dose atrial natriuretic factor enhances albumin escape from the systemic but not the pulmonary circulation. *Circ. Res.* **67**:461–468.
19. Renkin, E.M., and Tucker, V.L. 1996. Atrial natriuretic peptide as a regulator of transvascular fluid balance. *News Physiol. Sci.* **11**:138–143.
20. Leitman, D.C., et al. 1986. Identification of multiple binding sites for atrial natriuretic factor by affinity cross-linking in cultured endothelial cells. *J. Biol. Chem.* **261**:11650–11655.
21. Draijer, R., Atsma, D.E., van der Laarse, A., and van Hinsbergh, V.W. 1995. cGMP and nitric oxide modulate thrombin-induced endothelial permeability. Regulation via different pathways in human aortic and umbilical vein endothelial cells. *Circ. Res.* **76**:199–208.
22. Suttorp, N., Hippenstiel, S., Fuhrmann, M., Krull, M., and Podzuweit, T. 1996. Role of nitric oxide and phosphodiesterase isoenzyme II for reduction of endothelial hyperpermeability. *Am. J. Physiol.* **270**:C778–C785.
23. Westendorp, R.G., Draijer, R., Meinders, A.E., and van Hinsbergh, V.W. 1994. Cyclic-GMP-mediated decrease in permeability of human umbilical and pulmonary artery endothelial cell monolayers. *J. Vasc. Res.* **31**:42–51.
24. He, P., Zeng, M., and Curry F.E. 1998. cGMP modulates basal and activated microvessel permeability independently of $[Ca^{2+}]_i$. *Am. J. Physiol.* **274**:H1865–H1874.
25. Holtwick, R., et al. 2002. Smooth muscle-selective deletion of guanylyl cyclase-A prevents the acute but not chronic effects of ANP on blood pressure. *Proc. Natl. Acad. Sci. U. S. A.* **99**:7142–7147.
26. Kisanuki, Y.Y., et al. 2001. Tie2-Cre transgenic mice: a new model for endothelial cell-lineage analysis in vivo. *Dev. Biol.* **230**:230–242.
27. Isermann, B., et al. 2001. Endothelium-specific loss of murine thrombomodulin disrupts the protein C anticoagulant pathway and causes juvenile-onset thrombosis. *J. Clin. Invest.* **108**:537–546. doi:10.1172/JCI200113077.
28. Vicent, D., et al. 2003. The role of endothelial insulin signaling in the regulation of vascular tone and insulin resistance. *J. Clin. Invest.* **111**:1373–1380. doi:10.1172/JCI200315211.
29. Dubois, S.K., Kishimoto, I., Lillis, T.O., and Garbers, D.L. 2000. A genetic model defines the importance of the atrial natriuretic peptide receptor (guanylyl cyclase-A) in the regulation of kidney function. *Proc. Natl. Acad. Sci. U. S. A.* **97**:4369–4373.
30. Sultanian, R., Deng, Y., and Kaufman, S. 2001. Atrial natriuretic factor increases splenic microvascular pressure and fluid extravasation in the rat. *J. Physiol.* **533**:273–280.
31. Andrew, P.S., and Kaufman, S. 2003. Guanylyl cyclase mediates ANP-induced vasoconstriction of murine splenic vessels. *Am. J. Physiol.* **284**:R1567–R1571.
32. Takubo, K., Miyamoto, H., Imamura, M., and Tobe, T. 1999. Morphology of the human and dog spleen with special reference to intrasplenic microcirculation. *Jpn. J. Surg.* **16**:29–35.
33. Deng, Y., and Kaufman, S. 1996. Influence of atrial natriuretic factor on fluid efflux from the splenic circulation of the rat. *J. Physiol.* **491**:225–230.
34. Blackburn, R.E., Samson, W.K., Fulton, R.J., Stricker, E.M., and Verbalis, J.G. 1995. Central oxytocin and ANP receptors mediate osmotic inhibition of salt appetite in rats. *Am. J. Physiol.* **269**:R245–R251.
35. Garbers, D.L., and Dubois, S.K. 1999. The molecular basis of hypertension. *Annu. Rev. Biochem.* **68**:127–155.
36. Kishimoto, I., Dubois, S.K., and Garbers, D.L. 1996. The heart communicates with the kidney exclusively through the guanylyl cyclase-A receptor: acute handling of sodium and water in response to volume expansion. *Proc. Natl. Acad. Sci. U. S. A.* **93**:6215–6219.
37. Schubert, W., et al. 2002. Microvascular hyperpermeability in caveolin-1 (–/–) knock-out mice. Treatment with a specific nitric-oxide inhibitor, L-NAME, restores normal microvascular permeability in Cav-1 null mice. *J. Biol. Chem.* **277**:40091–40098.
38. He, P., Zeng, M., and Curry, F.E. 2000. Dominant role of cAMP in regulation of microvessel permeability. *Am. J. Physiol.* **278**:H1124–H1133.
39. Smolenski, A., Poller, W., Walter, U., and Lohmann S.M. 2000. Regulation of human endothelial cell focal adhesion sites and migration by cGMP-dependent protein kinase I. *J. Biol. Chem.* **275**:25723–25732.
40. Perticone, F., Maio, R., Tripepi, G., and Zoccali, C. 2004. Endothelial dysfunction and mild renal insufficiency in essential hypertension. *Circulation.* **110**:821–825.